Reentrant synclinic phase in an electric-field–temperature-phase diagram for enantiomeric mixtures of an antiferroelectric liquid crystal

Neha M. Patel and Charles Rosenblatt*
Department of Physics, Case Western Reserve University, Cleveland, Ohio 44106-7079, USA

Yi-kuo Yu
Department of Physics, Florida Atlantic University, Boca Raton, Florida 33431, USA
and National Center for Biotechnology Information, National Library of Medicine, National Institutes of Health, Bethesda, Maryland 20892, USA

(Received 19 February 2003; published 14 July 2003)

The threshold electric field E_{th} for a transition from the anticlinic to the synclinic phase of enantiomeric mixtures of the liquid crystal TFMHPOBC was measured as a function of temperature T and enantiomeric excess X. For small X the phase boundary curve on a temperature–electric-field phase diagram exhibits the phase sequence synclinic–anticlinic–reentrant synclinic on decreasing the temperature. At one point along the curve the quantity $dT/dE \rightarrow \infty$. For large values of enantiomeric excess a reentrant phase is not observed. The results are discussed using a simple phenomenological theory that accounts for layer-layer interactions, such that the electric-field-induced transition to the synclinic phase, although completed by solitary-wave propagation, is facilitated by a percolation mechanism.

DOI: 10.1103/PhysRevE.68.011703 PACS number(s): 61.30.Gd

The phenomenon of reentrant phases is exhibited by a diverse class of condensed matter systems. The monotonic variation of a thermodynamic field such as temperature T or electric field E may result in three phases in which the first and last phases possess the same symmetry. For liquid crystals this phenomenon was observed first as a nematic–smectic-A–nematic phase sequence (also denoted by N–Sm-A–N) with decreasing temperature in a mixture of alkoxycyanobiphenyls [1]. More recently a smectic-C^*–smectic-C_A^*–smectic-C^* phase sequence (also denoted by Sm-C^*–Sm-C_A^*–Sm-C^*) was observed on decreasing temperature for certain homologs of an anticlinic compound [2], where the asterisk signifies that the molecule is chiral. This phase sequence also has been observed on cooling in thin films that are subjected to an applied electric field [3,4].

For both the anticlinic (Sm-C_A^*) and synclinic (Sm-C^*) phases, the director $\hat{n}$ tilts by a polar angle θ with respect to the smectic layer normal. For molecules lacking inversion symmetry, this tilt induces a spontaneous polarization locally perpendicular to the tilt plane [5]. In the synclinic Sm-C^* phase the azimuthal angle φ_j is nearly identical in every layer j, with only a slight variation due to the chiral-induced long wavelength helix [6]. Thus, the polarization vectors in adjacent layers are nearly parallel. In the anticlinic Sm-C_A^* phase the director's azimuthal orientation alternates by approximately π from one layer to the next, and therefore the polarization vectors in adjacent layers are nearly antiparallel. Analogous to the helical structure of the synclinic phase, the azimuthal orientations φ_j and φ_{j+2} in the anticlinic phase differ slightly, resulting in a pair of commensurate long wavelength chiral helices: One helix is associated with the odd-numbered smectic layers and the other is associated with the even layers [6]. Anticlinic liquid crystals may exhibit tristable behavior [7] and can be switched from the anticlinic to synclinic configuration by a moderate electric field applied parallel to the layer plane. This switching has been observed to occur via fingerlike solitary waves of the synclinic phase that invade the anticlinic phase [8].

In this paper we report on measurements of the threshold field for a transition from the anticlinic to the synclinic phase of the liquid crystal TFMHPOBC (Fig. 1) [9] as a function of temperature and enantiomeric excess. The phase diagram at $E=0$ for TFMHPOBC is rather simple: For enantiomeric excess $X \gtrsim 0.6$, where $X \equiv ([r]-[s])/([r]+[s])$ and $[s]$ and $[r]$ are the molar concentrations of the left- and right-handed enantiomers, respectively, there is a direct transition from the Sm-A phase to the anticlinic Sm-C_A^* phase. For $X \lesssim 0.6$, a synclinic Sm-C^* phase appears between Sm-A and Sm-C_A^* phases. Our central result is the observation of a reentrant synclinic phase in the T-E phase diagram for $X < 0.42$; for larger values of enantiomer excess, the reentrant phase is preempted by a crystalline transition and is not observed. The results are examined theoretically in terms of competing ordering mechanisms.

Binary mixtures of left- and right-handed TFMHPOBC enantiomers were prepared by dissolving appropriate concentrations of the enantiomers in chloroform and evaporating the solvent at 50 °C for one day. Sample cells were constructed with two glass slides coated with semitransparent and electrically conducting indium tin oxide (ITO), thereby forming a capacitor-type cell. The ITO surfaces were cleaned and then spin coated with the polyimide RN1266 (Nissan Chemical) and baked at 250 °C for 60 min. The polyimide-coated surfaces then were rubbed uniformly with a cotton

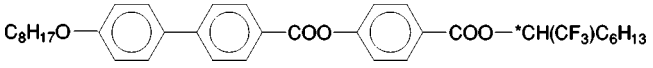

FIG. 1. Structure of TFMHPOBC.

*Corresponding author. Email: rosenblatt@cwru.edu

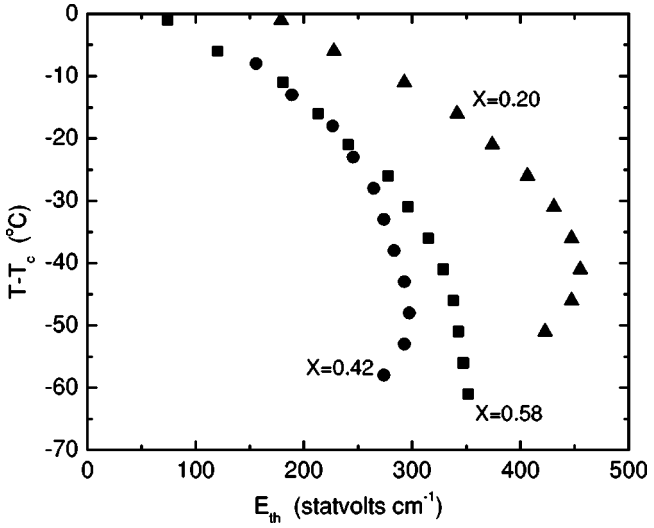

FIG. 2. Phase boundary curves. T_c is the upper Sm-C^*–Sm-C_A^* phase transition temperature at $E=0$, corresponding to $T_c=101\,^\circ$C for $X=0.20$, $108\,^\circ$C for $X=0.42$, and $111\,^\circ$C for $X=0.58$.

cloth using a rubbing machine to promote planar alignment of the liquid crystal. Finally, the slides were placed together, separated by Mylar spacers and cemented. The empty cell was mounted in a computer-controlled hot stage and was filled with the liquid crystal in the isotropic phase. The sample was then cooled into the Sm-C_A^* phase in the presence of a 10 Hz bipolar square-wave electric field with an amplitude of several volts per micrometer. The sample and hot stage were placed on a rotatable stage of a polarizing microscope and observed under crossed polarizers. In the anticlinic phase the sample was rotated until the image became dark—this is where the smectic layer normal is parallel to the polarizer. The temperature of the sample was reduced in steps of 5 °C until the onset of the crystalline phase. At each temperature step a 1 Hz monopolar square-wave electric field was applied perpendicular to the plane of the sample. The amplitude of the square wave, which was monitored by an oscilloscope, was ramped until bright, fingerlike solitary waves began to invade the dark anticlinic region, indicating a transition to the synclinic phase. The threshold electric field E_{th} corresponds to V_{th}/d, where V_{th} is the threshold voltage for the onset of fingering and d is the thickness of the cell determined by optical interferometry. The thickness d was found to be 4.1 ± 0.1 μm, 7.1 ± 0.1 μm, and 7.2 ± 0.1 μm for the $X=0.2$, 0.42, and 0.58 cells, respectively. We note that there was no apparent difference in the appearance of the regular synclinic phase and the reentrant synclinic phase. For sufficiently high electric field it was possible to go continuously from the higher temperature Sm-C^* phase to the reentrant Sm-C^* phase along an appropriate path in the T-E phase diagram.

The phase boundary curves for different values of enantiomeric excess are plotted in Fig. 2, where T_c is the concentration-dependent smectic-C^*–smectic-C_A^* transition temperature. The data reveal several features. First, for the two smaller values of X a reenetrant Sm-C^* phase was observed at lower temperatures. Notice that the slope $|dT/dE|\rightarrow\infty$ at a particular point on each phase boundary curve, which we shall designate by $E^\infty(X)$ and $T^\infty(X)$. Below this temperature, of course, the sign of dT/dE becomes positive. For the largest value of X, viz., $X=0.58$, the magnitude $|dT/dE|$ becomes larger at lower temperatures, but never changes sign. It is important to note that a crystalline phase sets in just below the lowest reported experimental temperature for each value of enantiomer excess, and thus it no longer was possible to examine the reentrant transition below this temperature. From Fig. 2 we note that the threshold fields for a given value of $T-T_c$ are not monotonic in X. This is because the polarization increases linearly with X, and also depends upon θ. [As observed in Ref. [10], the behavior *would* be monotonic in X if the phase boundary curves were plotted vs the quantity PE, where P is the average dipole moment per volume, which depends on both X and $\theta(T)$.]

At this point it is useful to consider the physical bases of the anticlinic and synclinic phases. Based on the molecular model of Osipov and Fukuda [11], the synclinic Sm-C^* phase is stablized relative to the anticlinic Sm-C_A^* phase by steric interactions and dispersive forces. On the other hand, a predominant feature of compounds that exhibit the Sm-C_A^* phase is that the molecules have a large transverse dipole moment located in the alkyl chain close to the end of the molecule. The Sm-C_A^* phase is believed to be stabilized by θ-dependent–and therefore temperature-dependent–orientational correlations of these transverse dipoles located in the adjacent smectic layers. Additionally, the free energy of the tilted smectic phases has temperature-dependent contributions from intralayer interactions between molecules in the same layer, from partial penetration of molecules from one layer into an adjacent layer, and from conformational and orientational order parameter correlations between neighboring molecules. This latter effect includes the possibility of local biaxial correlations. Because the energetics of the synclinic and anticlinic phases are rather similar, coupling of two or more interactions may lead to a reentrant Sm-C^* phase.

One explanation for reentrant behavior was offered by Pociecha *et al.* [2]. On examining the phase behavior as a function of temperature and homolog number (rather than electric field), they suggested that at lower temperatures quadrupolar ordering affects the interlayer interactions. This may give rise to local nematiclike biaxial ordering within a smectic layer, which, in turn, may facilitate interlayer penetration of molecules, promoting the reentrant synclinic phase at the expense of the anticlinic phase because $\varphi_j\approx\varphi_{j+1}$. Although such interactions may play a role in our system, we need to examine more closely the behavior that arises from mixtures of enantiomers. As seen in Fig. 2, reentrant synclinic behavior is *least* likely to occur for large X, i.e., for samples of higher optical purity. For these mixtures rr pairings of molecules in adjacent layers predominate because of the much smaller fraction of s enantiomers present in the mixture. It has been suggested [10,12] that the dipole moments for rr (or equivalently ss) pairings are antiparallel

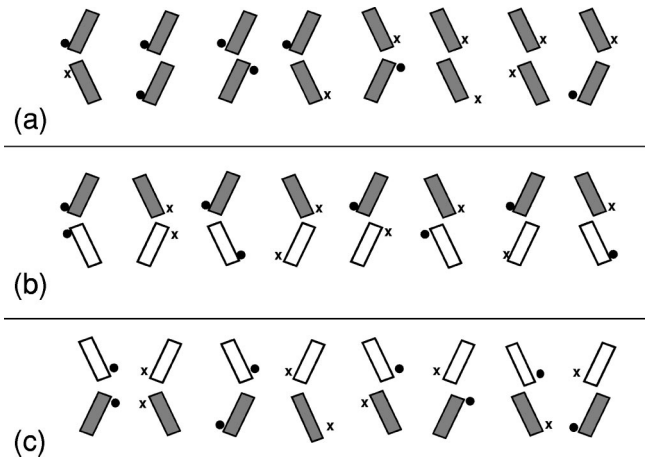

FIG. 3. Schematic representation of possible molecular pairings for (a) *rr* pairs, (b) *rs* pairs, and (c) *ss* pairs. *r* enantiomers are respresented by solid rectangles and *s* enantiomers by open rectangles. Dipole moments are represented by a dot (out of paper) or a cross (into paper). (a) corresponds to eight possible *rr* (or *ss*) pairings, (b) corresponds to *rs* pairings, and (c) corresponds to *sr* pairings.

in the anticlinic phase [Fig. 3(a)], and therefore are energetically favored. Thus, an optically pure material in which all interlayer pairings are of the *rr* (or *ss*) type is more likely to have an anticlinic Sm-C_A^* phase than would a racemic mixture, in which there would be many *rs* pairings that favor synclinic order [10,12]. This behavior was borne out in our earlier measurements of E_{th} in enantiomeric mixtures of TFMHPOBC at higher temperatures, where we inferred a slight biasing of *rr* and *ss* pairings over *rs* and *sr* pairings in the anticlinic phase [10]. Turning to the measurements presented herein, for the $X=0.58$ mixture the preponderance of *rr* pairings (due to the high fraction of *r* enantiomer) tends to inhibit the formation of a synclinic Sm-C^* phase. On the other hand, because *rs* pairings statisically are more likely to occur in the lower enantiomeric excess mixtures ($X=0.20$ and $X=0.42$), these mixtures have a smaller tendency to form an anticlinic Sm-C_A^* phase, promoting a Sm-C^* phase at temperatures above the Sm-C_A^* region.

But why should *reentrant* Sm-C^* behavior occur at lower temperatures for a given electric field? We offer a simple model that is based on two dominant interactions: (1) microscopic dipolar interactions, and (2) steric hindrance and/or nematiclike orientational interactions. We note that the microscopic dipolar interactions could be significantly different for *rr* (or *ss*) pairs vs *rs* pairs due to the chiral molecular structure. This asymmetry in the dipolar interactions is important, as will be seen below. For purposes of our model, we interpret the electric field-driven transition from Sm-C_A^* to Sm-C^* phase as a percolationlike phenomenon of Sm-C^* regions; these are seeded by the rodlike pairings. Physically, this peroclation corresponds to an azimuthal reorientation of molecules in the odd (or even) numbered layers, which inherently is a second-order process. Once these regions percolate locally, kinetic mechanisms complete the growth of the solitary waves. This overall process is reminiscent of the

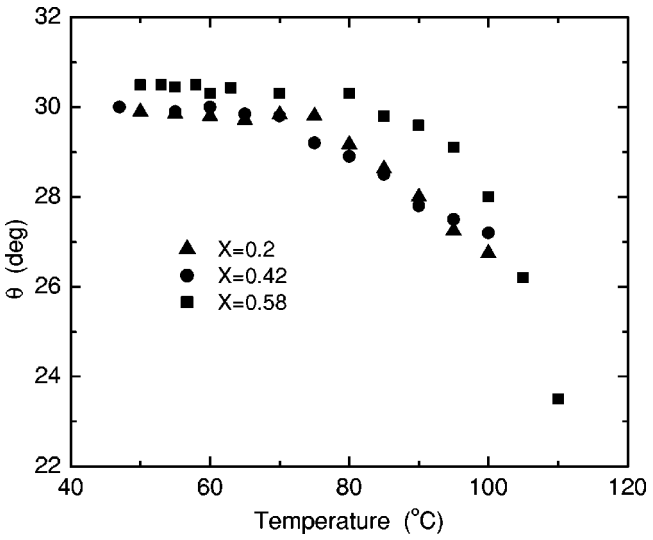

FIG. 4. Measured polar tilt angle θ_i vs T.

coalesence of ferromagnetic domains below the Curie temperature T_{Curie}. Upon the application of a weak magnetic field H, many of the weakly pinned domains merge to form still larger domains, and larger domains emerge through domain wall propagation. Although the temperature axis below T_{Curie} on a T-H magnetic phase diagram generally is referred to as a ''first-order transition line'' [13], the quantity dT/dH, which is associated with the reorientation of the magnetization vector in the presence of a magnetic field, actually is infinite everywhere along this line. Such behavior is not shared by typical first-order phase transitions such as the liquid-solid transition. Although our system is complicated by strong layer-layer interactions, dT/dE still may be infinite at a point on the line separating the antiferroelectric and ferroelectric phases, thereby resulting in a reentrant Sm-C^* phase at lower temperatures.

In order to include only the simplest ingredients, we assume complete mixing of enantiomers, i.e., X is spatially uniform. This is reasonable for small X and avoids the complications of microphase separation, thus allowing us to discuss the system using only temperature and electric fields as variables. The fraction of right-handed molecules is $(1+X)/2$ and the fraction of the left-handed molecules is $(1-X)/2$. Consequently, the fraction of *rr* pairings is $(1+X)^2/4$, the fraction of *ss* pairings is $(1-X)^2/4$, and the fraction of *rs* pairings is $2(1-X^2)/4$.

For a given dimer pair in which the two molecular dipoles are close together, the dipolar interaction energy is $U_0(\theta)=-U_0/\cos^3\theta$ for antiparallel dipole moments and $U_0(\theta)=+U_0/\cos^3\theta$ for parallel dipole moments (see Fig. 3), where U_0 is positive. Here the angle θ is the measured polar tilt angle (see Fig. 4) obtained by rotating the sample on a polarizing microscope stage to extinguish the transmitted light when the applied field ($|E|>E_{th}$) is reversed. The factor $\cos^3\theta$ comes from the fact that the spacing r_{ij} between the dipoles in layers i and j is proportional to $\cos\theta$ and the dipolar field is proportional to $1/r_{ij}^3$. (Note that Osipov and Fukuda [11] use a $1/r^6$ potential, which is appropriate for an idealized Sm-C_A^* phase in which inside each layer the dipole

moments are perpendicular to the molecular tilt plane and are translationally invariant, i.e., homogenized. In our case we consider individual microscopic *pairs*, giving us a $1/r^3$ potential.) When the dipoles in a given pair are far apart we assume that their interaction energy is negligible. For rr pairs the energy $-U_0/\cos^3\theta$ comes from a "bent" (Sm-C_A^*) configuration and $+U_0/\cos^3\theta$ from a rodlike (Sm-C^*) configuration; for rs pairs the energy $-U_0/\cos^3\theta$ comes from a rodlike configuration and $+U_0/\cos^3\theta$ from a bent configuration (see Fig. 3).

On examining the molecular structure, we find that rs rodlike pairings have less steric hindrance because the bent chiral tails can accomodate each other better in terms of their orientation. Therefore, the appearance of the synclinic Sm-C^* phase at high temperature in part is due to a reduction in steric hinderance and in part due to nematic orientational effects. At high temperature we, therefore, require that an additional negative energy term be associated with rs rodlike pairings. These effects are less important at low temperature where empirically the stable phase in the absence of an electric field is the anticlinic Sm-C_A^* phase. Thus, we introduce a single phenomenological energy term *that applies to rodlike rs pairings only* and that incorporates a simple temperature dependence to account for the synclinic propensity at high temperature and anticlinic propensity at low temperature, viz., $U_1(X,\theta)=a(1-X^2)(T_0-T)U_0\sin^4\theta$. Here T_0 is an appropriate empirical temperature for the crossover in sign, a is a positive constant, the θ-dependence derives from the S^2 interaction in the Maier-Saupe nematic mean-field theory, and $(1-X^2)$ is an averaging factor due to the presence of nearby anticlinic pairs; this factor mimics the vanishing of the effect when $X\rightarrow 1$. This form, of course, is a very crude approximation, although it bypasses the need for explaining the Sm-C_A^* to Sm-C^* transition in the absence of an electric field. Note that U_1 favors rodlike rs pairings at temperatures above T_0, whereas below T_0 it indirectly favors the bent rs configuration, i.e., the Sm-C_A^* phase, in the absence of an electric field. This is because at low temperature U_1 becomes positive and therefore *disfavors* the rodlike rs pairings, leaving only the bent pairings. Turning now to other interactions, intralayer nematiclike interactions are similar for both rodlike and bent pairings, and are denoted by $K(T)$. $K(T)$ has an important effect in the overall entropy of the phases, but is not the dominant factor for reentrant phenomena, rather it is the temperature at which $a(T_0-T)$ changes sign that most affects the reentrant behavior. For our data we chose $T_0 \approx 85\,^\circ\mathrm{C}$ for our calculations, which is in the middle range of the upper part of the phase boundary curves.

Let us now return to Fig. 3, which represents eight possible configurations each for rr, rs, and ss pairings. We assume that there is an electric field directed into the paper and that the dipoles are either parallel or antiparallel to the field. For this calculation we neglect effects due to the helical pitch, which is partially unwound by the electric field. In terms of our simple model, we can calculate the partition function for the dimers composed of these three types of pairings.

For the eight configurations of the rr pairings shown in Fig. 3(a), the energies are $-U_0(\theta)$, $2pE$, $2pE+U_0(\theta)$, 0, $-U_0(\theta)$, $-2pE$, $-2pE+U_0(\theta)$, and 0. Here $p=7\times10^{-19}$ esu cm is a molecular dipole moment appropriately averaged over conformations, orientations, and position. This value for p is obtained by scaling the polarization of the enantiomer in Ref. [9] by $M/\rho A\theta$, where $M=612\ \mathrm{g\,mol^{-1}}$ is the molecular weight of TFMHPOBC, ρ is the density (assumed to be $1\ \mathrm{g\,cm^{-3}}$), A is the Avogadro number, and θ is taken from Fig. 4. On including the intralayer nematic contribution K, the phenomenological rr partition function is

$$Z_{rr}=2e^{-\beta K}(e^{\beta U_0}+1)+e^{-\beta K}(e^{2\beta pE}+e^{-2\beta pE})(1+e^{-\beta U_0})$$
$$=2e^{-\beta K}(1+e^{-\beta U_0})[e^{\beta U_0}+\cosh(2\beta pE)], \quad (1)$$

where the polar tilt angle dependence and temperature dependence of the functions U_0 and U_1 are implied. The Lagrange multiplier β is analogous to $1/k_BT$ of the canonical ensemble, where k_B is the Boltzmann constant. However, because our phenomenological energy parameters depend on temperature, β, in principle, can have a very complicated dependence on temperature and need not necessarily correspond to $1/k_BT$. Nevertheless, we find that the approximation $\beta\equiv 1/k(T-T_f)$ seems reasonable, where T_f is the freezing temperature of the three types of pairings and k is a constant of magnitude similar to k_B. Note that T_f is the analog of $T=0$ for the ideal gas system. We find that when T_f falls in the temperature range $270<T<300$ K, no significant difference in the result is found. Note that the term $\cosh(2\beta pE)$ comes from the sum of the Boltzmann weights for the rodlike arrangement. The ss partition function $Z_{ss}=Z_{rr}$. For the rs pairings, the eight energy contributions are $U_0(\theta)+2pE$, $U_0(\theta)-2pE$, $2pE$, $-2pE$, $-U_0(\theta)+U_1(\theta)$, $-U_0(\theta)+U_1(\theta)$, $U_1(\theta)$, $U_1(\theta)$, and the partition function Z_{rs} is

$$Z_{rs}=2e^{-\beta K}(1+e^{-\beta U_0})[e^{\beta(U_0-U1)}+\cosh(2\beta pE)]. \quad (2)$$

Here the $\cosh(2\beta pE)$ term comes from the bent pairings. Additionally, the U_1 term, which applies only to rs pairings, appears in Z_{rs}.

As discussed above, the total fraction of rr and ss pairings is $(1+X^2)/2$ in the complete mixing approximation. Similarly, the fraction of rs pairings is $(1-X^2)/2$. If N is the total number of pairs, then $(1+X^2)N/2$ pairs are either rr or ss. Similarly, $(1-X^2)N/2$ is the number of rs pairs. Of the $(1+X^2)N/2$ pairs that are rr and ss, the number of rodlike pairs is

$$N_{rr}^{rod}+N_{ss}^{rod}$$
$$=N\frac{1+X^2}{2}\frac{2e^{-\beta K}(1+e^{-\beta U_0})\cosh(2\beta pE)}{2e^{-\beta K}(1+e^{-\beta U_0})[e^{\beta U_0}+\cosh(2\beta pE)]}$$
$$=\frac{N(1+X^2)}{2}\frac{\cosh(2\beta pE)}{e^{\beta U_0}+\cosh(2\beta pE)}.$$

Similary, the number of rodlike rs pairs is

$$N_{rs}^{rod}=\frac{N(1-X^2)}{2}\frac{e^{\beta(U_0-U_1)}}{e^{\beta(U_0-U_1)}+\cosh(2\beta pE)}.$$

From Eqs. (1) and (2) we obtain the fraction f^{rod} of rodlike pairs, which is equal to $N_{rr}^{rod}+N_{ss}^{rod}+N_{rs}^{rod}$ divided by the total number of pairs N. Thus

$$f^{rod}=\frac{1+X^2}{2}\frac{\cosh(2\beta pE)}{e^{\beta U_0}+\cosh(2\beta pE)} + \frac{1-X^2}{2}\frac{e^{\beta(U_0-U_1)}}{e^{\beta(U_0-U_1)}+\cosh(2\beta pE)}. \quad (3)$$

In order for the electric field-induced synclinic Sm-C^* phase to form, rodlike pairings must percolate. Furthermore, if percolation occurs within a layer, it is almost guaranteed to occur in the third (layer-normal) direction as well because the three-dimensional percolation threshold, in general, is smaller than the two-dimensional threshold [14]. We shall take f_p as the critical fraction of rodlike pairs for the occurance of percolation. For a triangular lattice $f_p=0.5$ [14], or equivalently, f^{rod} must be greater than 0.5 for percolation of the Sm-C^* on application of an electric field. Using Eq. (3), we have calculated the phase boundary curves based on this percolation criterion for the three values of enantiomer excess examined experimentally; the results are shown in Fig. 5. It is clear from the figure that our results are in good qualitative agreement with the experimental data. First, we find that the value of $T^{\infty}(X)$ (the temperature at which $|dT/dE|\rightarrow\infty$) is higher for smaller X. Also consistent with experiment, $|d^2T/dE^2|$ is larger, i.e., the curvature is greater, for small X. For $X=0.58$ the experiment does not show reentrant behavior, consistent with the absence (or at most marginal occurance) of reentrant behavior calculated from the simple theory. Turning to the field $E^{\infty}(X)$ at which $|dT/dE|\rightarrow\infty$, both experiment and theory are in agreement in which E^{∞} is largest for $X=0.2$. The only apparent discrepancy between theory and experiment is the order of $E^{\infty}(X)$ for the middle and higher enantiomer excesses, although as noted above the complete mixing assumption is more likely to break down at higher enantiomer excess and alter the details of the transition.

To summarize, we have observed experimentally a reentrant synclinic phase in an electric-field–temperature-phase diagram. We have presented a ''bare bones'' phenomenological model that includes only the dipole-dipole interactions, pE interactions, and steric interactions in order to describe the behavior qualitatively. Interestingly, although at low temperatures the rodlike (synclinic) rs pairings are treated as unfavorable in our theory via the U_1 term, they drive the system into a reentrant synclinic phase instead of making the anticlinic phase more robust against external electric field. This indicates that our model, although necessarily over simplified, probably contains the necessary ingredients to describe the correct behavior. Future work will involve a more robust theory in which nematiclike orientational interactions, including biaxiality, and microphase separation are included, as well as experimental investigations of the kinetics of the transition, especially in the neighborhood of $E^{\infty}(X), T^{\infty}(X)$.

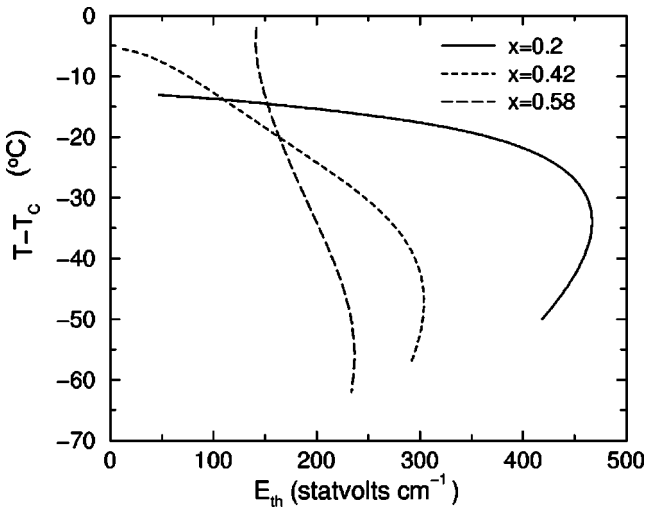

FIG. 5. The phase diagram from our simple theory. Parameter choices: $T_0=85\,^{\circ}$C, $T_f=280$ K, the microscopic dipole moment being 7×10^{-19} esu cm, as described in the text, $k=2.3\times10^{-16}$ erg/K, $U_0=5.75\times10^{-18}$ erg.

We thank Mohammad Reza Dodge and Ishtiaque M. Syed for experimental assistance and Dr. Tim Doerr for theoretical support. This work was supported by the National Science Foundation Solid State Chemistry program under Grant No. DMR-9982020.

[1] P.E. Cladis, Phys. Rev. Lett. **35**, 48 (1975).
[2] D. Pociecha, E. Gorecka, M. Cepic, N. Vaupotic, B. Zeks, D. Kardas, and J. Mieczkowski, Phys. Rev. Lett. **86**, 3048 (2001).
[3] C.Y. Chao, C.R. Lo, P.J. Wu, Y.H. Liu, D.R. Link, J.E. Maclennan, N.A. Clark, M. Veum, C.C. Huang, and J.T. Ho, Phys. Rev. Lett. **86**, 4048 (2001).
[4] P.J. Wu, C.Y. Chao, C.R. Lo, M. Veum, D.R. Link, J.E. Maclennan, and N.A. Clark, Ferroelectrics **277**, 511 (2002).
[5] R.B. Meyer, L. Liebert, L. Strzelecki, and P. Keller, J. Phys. (France) Lett. **36**, L69 (1975).
[6] Y.P. Panarin, O. Kalinovskaya, and J.K. Vij, Liq. Cryst. **25**, 241 (1998).
[7] A.D. L. Chandani, T. Hagiwara, Y. Suzuki, Y. Ouchi, H. Takazoe, and A. Fukuda, Jpn. J. Appl. Phys., Part 2 **27**, L729 (1988).
[8] J.F. Li, X.Y. Wang, E. Kangas, P.L. Taylor, C. Rosenblatt, Y. Suzuki, and P.E. Cladis, Phys. Rev. B **52**, 13 075 (1995).
[9] Y. Suzuki, T. Hagiwara, I. Kawamura, N. Okamura, T. Kitazume, M. Kakimoto, Y. Imai, Y. Ouchi, H. Takazoe, and A. Fukuda, Liq. Cryst. **6**, 167 (1989).
[10] M.R. Dodge and C. Rosenblatt, Phys. Rev. E **62**, 6891 (2000).
[11] M.A. Osipov and A. Fukuda, Phys. Rev. E **62**, 3724 (2000).
[12] T. Isozaki, H. Takezoe, A. Fukuda, Y. Suzuki, and I. Kawamura, J. Mater. Chem. **4**, 237 (1994).
[13] M. Schick, J.S. Walker, and M. Wortis, Phys. Rev. B **16**, 2205 (1977).
[14] D. Stauffer and A. Aharony, *Introduction to Percolation Theory*, 2nd ed. (Taylor and Francis, Philadelphia, 1994).